Comparison of two-typed (3-mercaptopropyl)trimethoxysilane-based networks on Au substrates

Yanfei Shen, Tian Wu, Yuanjian Zhang, Jinghong Li*

State Key Laboratory of Electroanalytical Chemistry, Changchun Institute of Applied Chemistry, Chinese Academy of Sciences, 159 People Street, Changchun 130022, China

Abstract

Two-typed (3-mercaptopropyl)trimethoxysilane-based networks which had been used to fabricate biosensors were prepared on Au substrates by two methods: layer-by-layer assembly, and the combination of sol–gel and self-assembly process. The formation mechanism and their surface properties, as well as stabilities were examined by cyclic voltammetry, electrochemical impedance spectroscopy, and X-ray photoelectron spectroscopy. It was found that the precursors formed bilayers with the thickness of ca. 1.8 nm on Au by layer-by-layer assembly only with −SH on the uppermost surface. The sol–gel and self-assembly processed multilayers with the thickness of ca. 6.8 nm and abundant −SH all over the network provided a rigid and stable network. Therefore, the coupling of sol–gel and self-assembly process provided a faster, simpler and more effective method to fabricate more rigid and stable networks; in this case, the local aqueous microenvironment as in biological media could preserve the native stabilities and reactivities of biological macromolecules better, which was expected to guarantee the high biological activity and stability of biosensors.
© 2004 Elsevier B.V. All rights reserved.

Keywords: Network; Self-assembly; (3-Mercaptopropyl)trimethoxysilane; Layer-by-layer; Sol–gel; Biosensor

1. Introduction

The development of biological immobilization has resulted in a large numbers of use of biomolecules for selective delivery, extraction, conversion, separation, and detection of reagents. The use of biological species such as peptides, proteins, and nucleic acids in these applications has typically relied in large part on the successful immobilization of the intact biological reagent onto or within a suitable surface [1–5]. The requirements for useful bioimmobilization include a high density of immobilized biomolecules, high activity, long-term stability under potentially adverse reaction conditions, good accessibility to analytes and rapid response time. The common conventional methods to immobilize biomolecules are typically based on physical adsorption, covalent binding to surfaces, entrapment in semi-permeable membranes and microencapsulation in polymer microspheres and hydrogels [6–9].

Self-assembly has become a popular surface derivatization procedure since its high organization and homogeneity make it very attractive for tailoring surfaces with desired properties. The modification includes not only growing monolayers but also growing multilayers on substrates. Conceptually, multilayer growth can take place due to the lack of self-limiting chemistry, that is, random growth, or due to well-defined monolayer growth, subsequent chemical modification of the monolayer surface, and then further monolayer growth [10]. The short-chain alkoxy silane molecular layers have a significant advantage over the other types of silanes in that they are the most widely available with the most diversity in their functional groups. In particular, (3-mercaptopropyl)trimethoxysilane (MPTMS) has been used as a heavy metal ion adsorbent [11–13], and for protein immobilization [14]. Recently, a three-dimensional network of MPTMS assembled onto gold electrodes has been

* Corresponding author. Tel.: +86 431 5262243; fax: +86 431 5262243.
  E-mail address: lijingh@ciac.jl.cn (J. Li).

used as gold nanoparticles adsorbent in biosensors, because this kind of surface structure provides efficient attaching sites for gold nanoparticles and a variety of biomolecules [15,16].

Park and Weaver proposed a simple method to prepare a three-dimensional network of MPTMS suited to adsorb a variety of nanoparticles [17]. The MPTMS monolayer was first assembled onto gold substrates via Au−S bond; then the methoxysilane units were hydrolyzed in NaOH and polymerized into a two-dimensional network; finally, a second silane layer was formed by immersing the modified substrates back into the MPTMS solution. The typical total time for the preparation was about more than 10 h. The resulting multilayers prepared based on layer-by-layer assembly were namely denoted as LbLMs in the following text (Scheme 1A). The gold nanoparticles immobilized on the thiol-terminated uppermost surface of LbLMs were near monolayer-level and demonstrated optimal electronic response between the nanoparticle arrays and the gold substrates. Moreover, biological macromolecules could retain their activity when adsorbed on gold nanoparticles [18,19]. This kind of network was expected to be attractive for the electrochemical biosensor development with excellent electrochemical and photochemical properties.

Mesoporous silicate materials can easily be prepared under ambient conditions using the sol–gel process [20]. One of the attractive features of sol–gel-derived materials is that they can be readily used as stable host matrixes for the entrapment of specific reagents such as proteins, enzymes, organic dyes, and redox probes [21–24]. Among numerous applications, sol–gel-derived materials have been used in solid-state electrochemical devices, chemical sensors, and catalysts [25–30]. Wang et al. designed a three-dimensional interfacial structure of MPTMS on a gold electrode via the direct coupling of sol–gel and self-assembly technologies for the first time [31]. The gold electrode was modified with the silica gel by immersing it in prehydrolyzed MPTMS sol for a desired time. The resulting multilayers on Au would be referred to as SGMs in the following text (Scheme 1B). Dong and co-workers proposed a new method to use the same interfacial structure on gold electrodes to fabricate a self-assembled nanoparticle biosensor by anchoring gold nanoparticles and further the enzymes [15]. The total preparation time of the SGMs on Au was optimized to be about 50 min. The sol–gel network was full of −SH, so that gold nanoparticles could be assembled both inside and on the surface of the network; thus it was expected to increase the biomolecules loading and promote detection limits and analytical ranges in biosensors.

Here, both of these three-dimensional self-assembled networks were attractive for electrochemical biosensors. Of utmost importance to this application is to understand the diffusivity and stability of the reagents trapped inside the silane networks [32,33]. Therefore, it was necessary to study their formation mechanism and compare their surface properties and stability to optimize the effective immobilization method of biological molecules. Herein, we focused on the comparative study about the surface properties and stability of the

three-dimensional MPTMS multilayers on gold electrodes by using cyclic voltammetry (CV), electrochemical impedance spectroscopy (EIS), and X-ray photoelectron spectroscopy (XPS).

2. Experimental

2.1. Reagents

(3-Mercaptopropyl)trimethoxysilane (MPTMS) (HS (CH$_2$)$_3$Si(OCH$_3$)$_3$) was obtained from Acros. K$_4$Fe(CN)$_6$, K$_3$Fe(CN)$_6$, ethanol and other reagents were of analytical grade and used as received. All aqueous solutions were prepared with double distilled water with a Millipore-Q system (18.2 MΩ).

2.2. Preparation of three-dimensional self-assembled networks of MPTMS on gold electrodes

A gold electrode was mechanically polished with 1, 0.3 and 0.05 μm α-Al$_2$O$_3$, washed ultrasonically with double distilled water, blown dry with nitrogen, and subsequently electrochemically cleaned in 1 M H$_2$SO$_4$ by potential scanning between −0.2 and 1.55 V until a reproducible cyclic voltammogram was obtained.

The general procedure for preparation of LbLMs [17] (Scheme 1A) involved three successive steps as follows: the self-assembly of MPTMS monomers to form a monolayer on the gold electrode via Au−S; the hydrolysis of the self-assembled monolayer and the polycondensation of the hydrolyzed monolayer; and forming the second MPTMS layer via Si−O−Si by immersing the modified electrode into the MPTMS solution once more. Briefly, the cleaned gold electrode was immersed in a 40 mM MPTMS in ethanol solution for 3 h, to produce self-assembled monolayers. After thoroughly rinsed, the silane units were polymerized into a 2D-network by dipping into 0.1 M NaOH for 2 h. A second silane layer was formed by immersion back into the MPTMS solution for another 3 h.

The sol–gel processes from MPTMS precursor occurred according to the sequence "hydrolysis–condensation" to get a three-dimensional framework: the hydrolysis of the precursors catalyzed by the presence of protons in the medium and the polycondension of the hydrolyzed monomers; and the self-assembly of the sol–gel MPTMS onto the gold electrode. The total time for preparation of SGMs [15] (Scheme 1B) was about 50 min, which was 10 more times shorter than that of LbLMs. In brief, silica sol was prepared by mixing MPTMS with water at a ratio of 1:4, 10 % (v/v) of ethanol, and 3.3 % (v/v) of 0.1 M hydrochloric acid. The mixture was sonicated for 30 min until a clear and homogeneous solution was obtained. The cleaned gold electrode was thoroughly rinsed with water and absolute ethanol, blown dry with nitrogen, and was immersed in the MPTMS sol–gel for 20 min at room temperature.
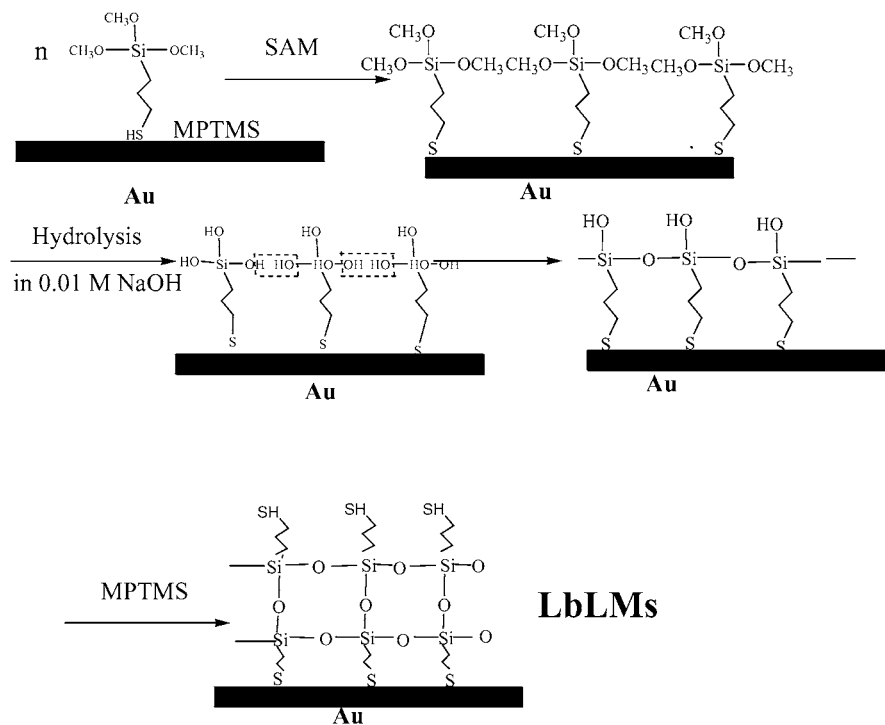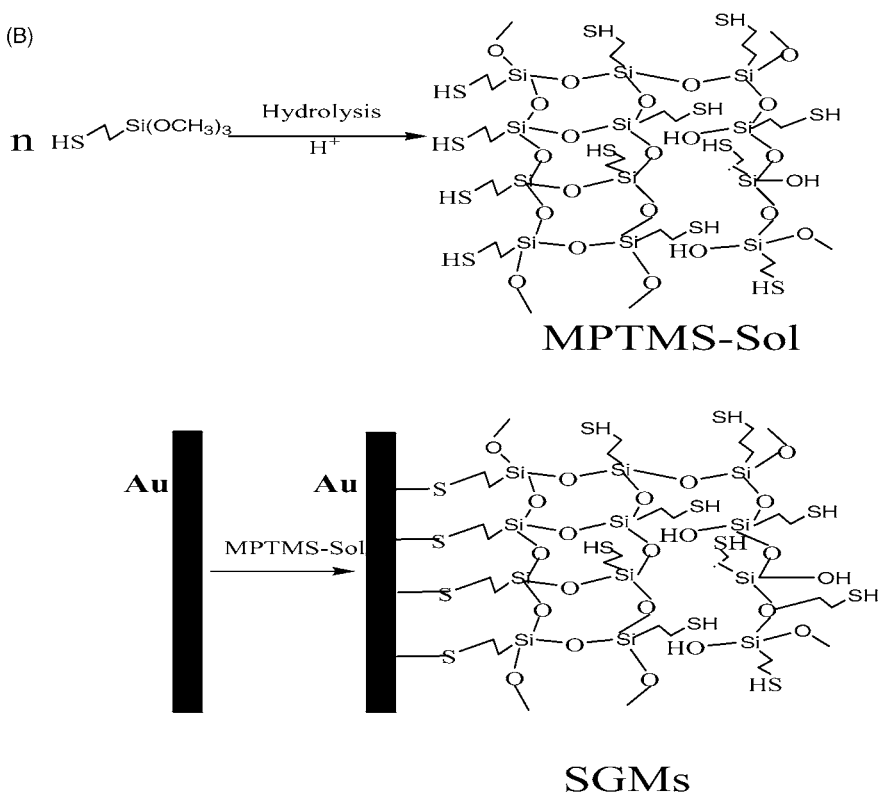
Scheme 1. The schematic illustration of the preparation processes of: (A) LbLMs and (B) SGMs on gold electrodes.

Both the resulted self-assembled electrodes were thoroughly rinsed with ethanol to remove physically adsorbed molecules and then blown dry with nitrogen. The LbLMs had thiol-terminated uppermost surface, which could be used for further assembly (Scheme 1A), and the SGMs were full of −SH both inside the network and on the surface (Scheme 1B), which could serve as a matrix for the encapsulation of a variety of molecules.

2.3. Instrumental

Electrochemical measurements were carried out in a conventional three-electrode electrochemical cell. The working electrode was a gold electrode, or, a LbLMs or SGMs modified electrode the auxiliary electrode was a platinum wire and the reference electrode was an Ag/AgCl (saturated KCl) electrode. Cyclic voltammetry measurements were performed with CHI 832 Electrochemical Instrument (CHI Inc., USA). EIS measurements were performed with a Solartron 1470 Battery Test Unit and a Solartron 1255 B Frequency Response Analyzer (Solartron Inc., England) for $5\,mM\ K_4[Fe(CN)_6]$ + $5\,mM\ K_3[Fe(CN)_6]$ in 0.1 M KCl aqueous solution. A sinusoidal potential modulation of $\pm 5\,mV$ amplitude was superimposed on the formal potential (0.22 V) of the redox couple of $[Fe(CN)_6]^{4-}/[Fe(CN)_6]^{3-}$. Applied frequency was from 10^6 to 0.1 Hz. The impedance data were fitted to an electrical equivalent circuit using the Z plot/Z view software (Scribner Associates Inc., England).

X-ray photoelectron spectroscopy (XPS) was conducted using a VG ESCALAB MK II spectrometer (VG Scientific, UK) employing a monochromatic Mg Kα X-ray source ($h\nu$ = 1253.6 eV). Peak positions were internally referenced to the C1s peak at 284.6 eV. Samples for XPS observation were prepared on gold plates with the same process as those on gold electrodes.

3. Results and discussion

Cyclic voltammetric blocking experiments, using ferrocyanide as a redox marker, could provide useful insights into the electron-transfer barrier properties of the MPTMS layers on gold electrodes [34,35]. Cyclic voltammograms of 5 mM $K_3Fe(CN)_6$ shown in Fig. 1 were obtained at: (a) the bare gold electrode (b) the LbLMs; and (c) SGMs modified electrodes, respectively. As a consequence of film formation on Au, the intensity of the well-defined peaks observed at the bare gold electrode was greatly diminished in the presence of the silica layers formed by layer-by-layer means, and the combination of the sol–gel and self-assembly process, which confirmed that MPTMS layers were successfully assembled on the gold surface in both cases. Moreover, the voltammetric response turned from peak-shaped signals to waves of sigmoidal form, suggesting the predominance of radial diffusion instead of the classical linear mode of mass transfer. This was due to the presence of a physical barrier limiting somewhat the probe diffusion through the film from the solution to the electrode surface. It seemed therefore that the modified electrode behaved as an ensemble of ultramicro-electrodes, which arised from the gold microareas defined by the porous structure of
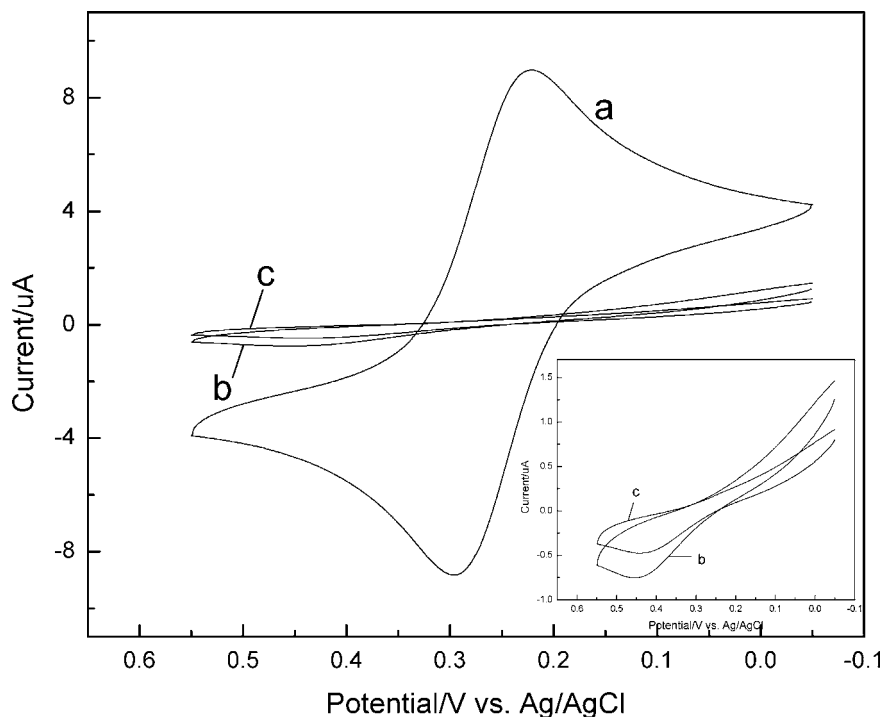

Fig. 1. Cyclic voltammograms of 5 mM $K_3[Fe(CN)_6]$ at: (a) bare gold electrode and (b) LbLMs; and (c) SGMs modified gold electrodes in the solution of 0.1 M KCl. Scan rate, 50 mV/s.

silica layers, as the case of the porous methylated silica films on ITO [36]. A little stronger barrier effects were observed for SGMs from curve c, indicating that the SGMs were thicker than the LbLMs.

In the last few years, impedance spectroscopy has become a widespread analytical tool to investigate the electrical properties such as dynamics of numerous systems. The main advantage of an electrochemical impedance spectroscopy (EIS) measurement is that it is a perturbation technique, that is, the initial state of the system remains unaltered by the measurement sequence. This technique is ideally suited for following a slowly changing system, as long as the difference between its initial and final state remains relatively small during the measurement period [37].

In order to investigate the stability of the MPTMS layers on gold electrodes prepared by two routes, we performed the EIS experiments measured at frequency intervals. Impedance measurements of 5 mM $K_4[Fe(CN)_6]$ + 5 mM $K_3[Fe(CN)_6]$ at MPTMS layers modified electrodes were carried out in the solution of 0.1 M KCl, as shown in Fig. 2. We used the equivalent circuit mold (Scheme 2) to simulate the complex impedance plots obtained from the EIS measurements. The curve (solid line in Fig. 3) fits well with the experimental impedance data (solid square in Fig. 3), which indicates that the equivalent circuit used is accurate. The semi-circle at the high frequencies represented the response of heterogeneous electron transfer kinetics. These are the relations below [38]:

$$R_{ct} = \frac{RT}{nFi_0} \qquad (1)$$

$$i_0 = nFAk^oC \qquad (2)$$

R_{ct}, the electron-transfer resistance; k^o, the electron transfer rate constant, could be obtained from formulae (1) and (2). The straight-line at the low frequencies was due to the diffusion of the redox couple in the solution. The diameters of the semi-circles represented the resistances of the layers, which could reflect their blocking capabilities for the redox couple. It was usually assumed that the electron transfer of $[Fe(CN)_6]^{4-}/[Fe(CN)_6]^{3-}$ was blocked by the formation of highly organized layers on the electrode surface because these redox species could hardly penetrate the layers into the conductive electrode surface. The value of k^o as an electrical barrier could be reflected by R_{ct} of the redox probe of $[Fe(CN)_6]^{4-}/[Fe(CN)_6]^{3-}$. All fitting results were presented in Table 1.

In Fig. 2A, the semi-circle diameter in the Nyquist plot seemed to gradually decrease along with time, generating a decrescent interfacial R_{ct} and weakened blocking to the electron transfer of the redox probe (Table 1A). The film thickness was calculated according to the following equations [38].

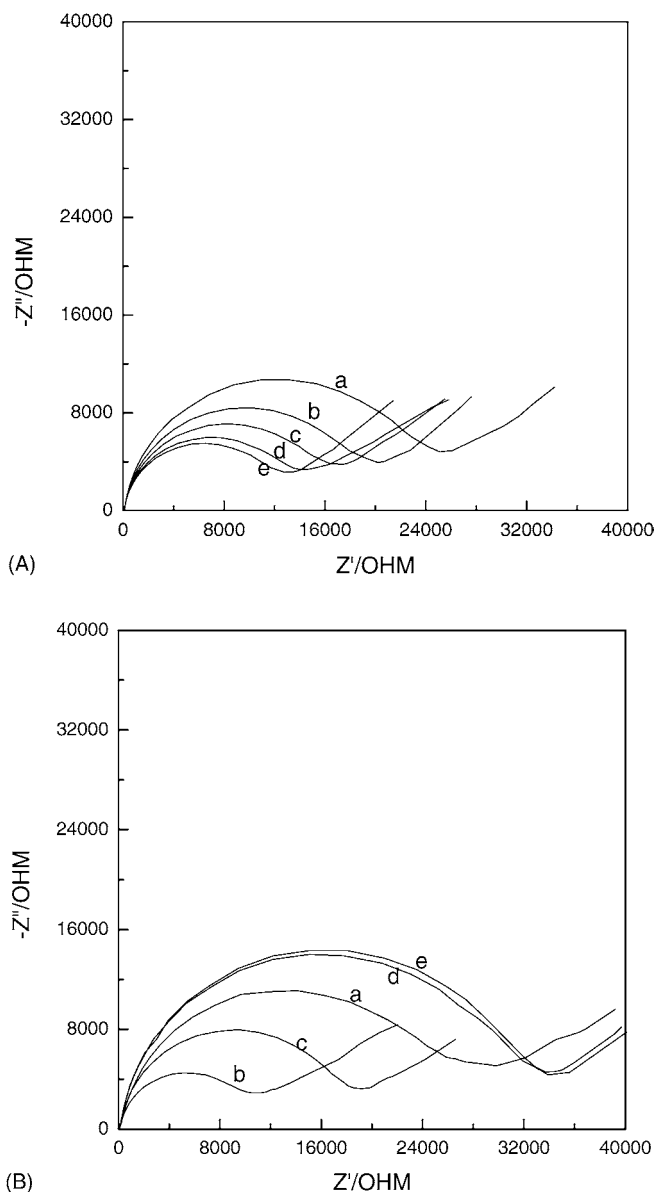$$C_m\theta + C_{bare}(1 - \theta) = C_{dl} \qquad (3)$$

(A)

(B)

Fig. 2. Electrochemical impedance spectroscopy results of 5 mM $K_4[Fe(CN)_6]$ + 5 mM $K_3[Fe(CN)_6]$ at (A) LbLMs and (B) SGMs modified gold electrodes in 0.1 M KCl at: (a) 0 h; (b) 1 h; (c) 2 h; (d) 3 h and (e) 4 h after preparation. A sinusoidal potential modulation of ±5 mV amplitude was superimposed on the formal potential of the redox couple of $[Fe(CN)_6]^{4-}/[Fe(CN)_6]^{3-}$ (0.22 V vs. Ag/AgCl) and the applied frequency was from 10^6 to 0.1 Hz.
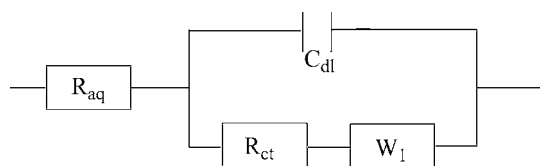
Scheme 2. Equivalent circuit mold for complex impedance plots. R_{aq}, the solution resistance; C_{dl}, the modified layer/solution interface capacitance; R_{ct}, the electron transfer resistance due to the electron transfer at the modified layer/solution interface; W_1, Warburg diffusion impedance due to the diffusion of the redox couple ($[Fe(CN)_6]^{4-}/[Fe(CN)_6]^{3-}$) in the solution.
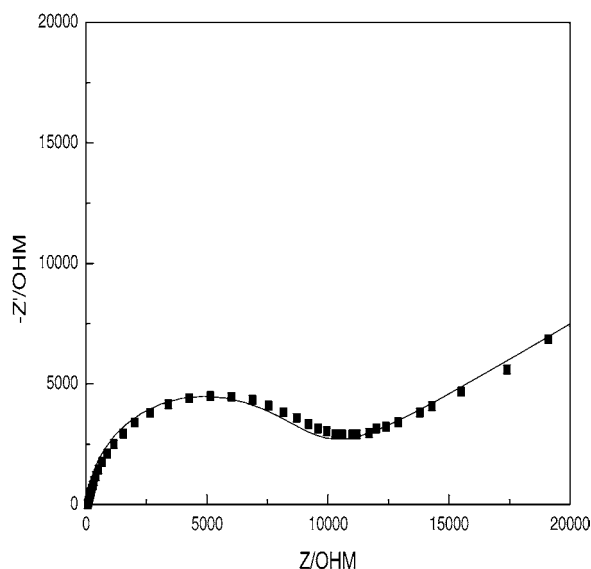
Fig. 3. Simulated result of SGMs/Au after 1 h by apllying the equivalent circuit in Scheme 2. The solid squares (■) represented the impedance plot and the solid lines (—) represented the simulated result of SGMs/Au after 1 h.

$$d = \frac{\varepsilon_m \varepsilon_0 A}{C_m} \qquad (4)$$

C_m, the film capacitance; C_{bare}, the double-layer capacitance in the pinhole; C_{dl}, the capacitance of the modified layer/solution interface; θ, the surface coverage; d, the film thickness; ε_m, the relative permittivity of the film; ε_0, the permittivity of vacuum; A, the electrode area. In the first 1 h, the LbLMs film thickness reduced rapidly, and then the change rate slackened gradually along with time (Table 1A). It might be that the physical absorbed MPTMS molecules were re-

moved from the porous structure of the LbLMs film. After 4 h, the thickness of the LbLMs on Au was calculated to be ca. 1.8 nm according to the EIS results, in agreement with twice the length of the MPTMS molecule, manifesting that MPTMS molecules formed successfully bilayers on Au by layer-by-layer assembly [39].

In Fig. 2B, the semi-circle diameter decreased at the beginning of the measurement, and then increased. A steady state reached after 4 h and did not change later (Table 1B). One possibility for the change was that the structure and properties of the gel on the gold surface continued to change because some silanols were maintained in the pores of the gel. At the early stage of preparation, polycondensation reactions continued to occur within the gel network as long as neighboring silanols were enough to react, creating more cross-linked structures and more pores. Therefore, during this stage, the charge transfer and diffusion of the $[Fe(CN)_6]^{4-}/[Fe(CN)_6]^{3-}$ became more and more easier and k^o increased rapidly. Then the syneresis process took place. During this process, the gel shrinked and the liquid was partially expulsed from the pores. It had been suggested by Hench and West that the contraction was driven by the tendency to reduce the solid–liquid interfacial area of the gel [40], which made the multilayer more compact. From comparison of the results of the impedance at the end of the experiment in Table 1, R_{ct} for SGMs was twice larger than that for LbLMs. The thickness was about 6.8 nm according to formulae (3) and (4), which could be that more than two layers of MPTMS molecules assembled on Au. It was in agreement with the expected higher thickness and compactness of SGMs, indicating that both the charge transfer and diffusion of the $[Fe(CN)_6]^{4-}/[Fe(CN)_6]^{3-}$ were more inhibited through SGMs than through LbLMs. These results indicated that the SGMs were thicker and more stable than LbLMs. Therefore, in biosensor applications, the stable silicate matrix of SGMs full of −SH could immobilize more encapsulated enzymes and prevent enzymes desorption, guaranteeing high biological activity and stability. As a result, the sol–gel from MPTMS provided a more stable network structure with more active sites for biomolecules, while the relatively unstable LbLMs with less thiol, which might restrict the biomolecules loading, would have a very limited dynamic range and low sensitivity.

X-ray photoelectron spectra (XPS) provided another pathway to investigate the film properties of the LbLMs and SGMs on gold surfaces (Fig. 4). These spectra indicated that MPTMS molecules were introduced to the gold surfaces. Comparing the Fig. 4a and b, it was found there was nearly no shift of elemental binding energy such as Si_{2p}, O_{1s} and S_{2p}. Howerer, the peak areas of Si_{2p}, O_{1s} and S_{2p} for SGMs are much larger than those for LbLMs; it indicated that SGMs were much thicker than LbLMs. Moreover, the peak at 85.3 eV, the feature of Au−S bond ($Au_{4f7/2}$) disappeared in the case of SGMs, indicating that SGMs on the gold surface were so thick that they blocked the XPS detection of Au_{4f}. Therefore, there were much
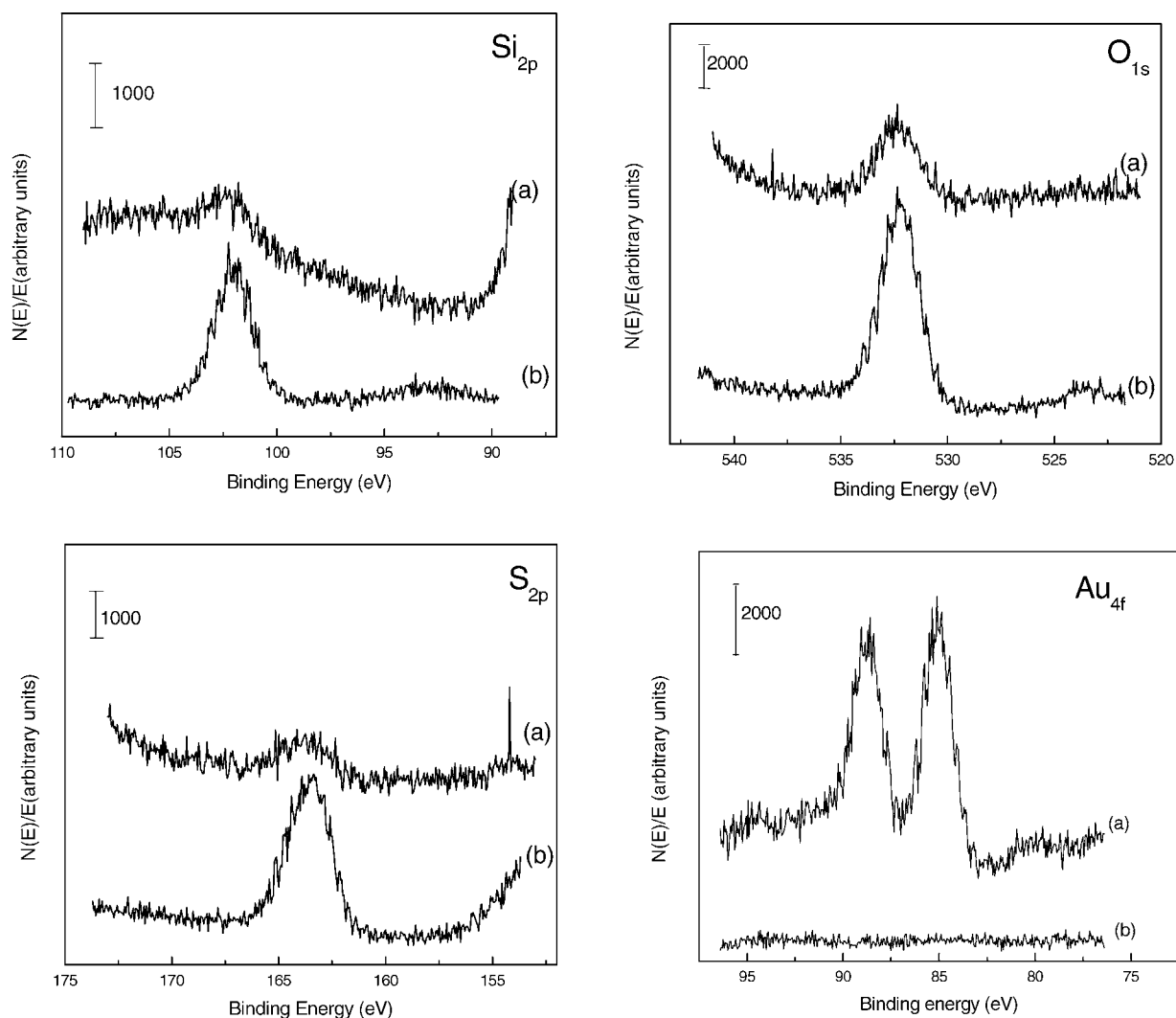
Table 1
The ac-impedance results of 5 mM $K_4[Fe(CN)_6]$/5 mM $K_3[Fe(CN)_6]$ at (A) LbLMs and (B) SGMs modified gold electrodes in the solution of 0.1 M KCl

Time (h)	0	1	2	3	4
(A)					
D (kΩ)	25.8	21.0	18.0	14.8	13.8
R_{ct} (kΩ)	21.5	17.5	14.2	12.0	10.5
C_{dl} (10^{-7} F)	2.03	2.44	2.58	2.63	2.65
d (nm)	2.34	1.94	1.84	1.81	1.79
k^o (10^{-7} m s^{-1})	7.88	9.68	11.90	14.10	16.10
					(B)
D (kΩ)	28.2	11.4	19.0	33.9	34.2
R_{ct} (kΩ)	22.4	7.6	14.8	29.0	30.0
C_{dl} (10^{-7} F)	1.66	1.99	1.81	1.62	1.62
k^o (10^{-7} m s^{-1})	7.57	22.40	11.45	5.84	5.65

A sinusoidal potential modulation of ±5 mV amplitude was superimposed on the formal potential of 0.22 V (vs. Ag/AgCl (saturated KCl)). Applied frequency was from 10^6 to 0.1 Hz. D, the diameter of the semicircle of EIS; d, the thickness of LbLMs; R_{ct}, the electron transfer resistance due to the electron transfer at the modified layer/solution interface; C_{dl}, the capacitance of the modified layer/solution interface; k^o, the electron transfer rate constant. The data are obtained from Fig. 2.

Fig. 4. High-resolution XPS spectra of the Si_{2p}, O_{1s}, S_{2p} and Au_{4f} for: (a) LbLMs and (b) SGMs on gold plates.

more specific functionalities such as −SH and Si−O−Si in SGMs which could be used to covalently bind biomolecules. Furthermore, the sol–gel host matrix could provide essentially the local biological aqueous microenvironment, which was well suitable for immobilization of biomolecules for sensing.

4. Conclusion

In summary, we compared the two methods of preparation for alternatively the three-dimensional networks of (3-mercaptopropyl)trimethoxysilane on Au substrates: one was layer-by-layer assembly, the other was the combination of sol–gel and self-assembly process. It was found that for the former (3-mercaptopropyl)trimethoxysilane molecules formed bilayers on Au with relatively finite thiol moieties on the uppermost surface, which might lead to low enzyme loading, and low detection sensitivity and efficiency in the application of biosensor. For the latter, the polycondension and syneresis processes occurred just after preparation, which made the intersectant network more stable, eliminating the charge transfer rate constant of the redox probe $K_4[Fe(CN)_6]/K_3[Fe(CN)_6]$ by less than three times compared to that at the LbLMs modified electrode. Therefore, the coupling of sol–gel and self-assembly process provided a relatively faster, simpler and more effective method to fabricate more stable networks, which could guarantee the higher biological activity and stability of biosensors, and would be widely employed in the applications of biosensors.

References

[1] T. Wink, S.J. vanZuilen, A. Bult, W.P. vanBennekom, Analyst 122 (1997) R43.

[2] S.K. Sharma, N. Sehgal, A. Kumar, Curr. Appl. Phys. 3 (2003) 307.

[3] J. Li, S.N. Tan, H.L. Ge, Anal. Chim. Acta 335 (1996) 137.

[4] S. Campuzano, B. Serra, M. Pedrero, F.J.M. de Villena, J.M. Pingarron, Anal. Chim. Acta 494 (2003) 187.

[5] D. Trau, R. Renneberg, Biosens. Bioelectron. 18 (2003) 1491.

[6] X.J. Wu, M.M.F. Choi, Anal. Chem. 75 (2003) 4019.

[7] C. Tlili, K. Reybier, A. Geloen, L. Ponsonnet, C. Martelet, H.B. Ouada, M. Lagarde, R.N. Jaffrezic, Anal. Chem. 75 (2003) 3340.

[8] M.D. Marazuela, M.C. Moreno-Bondi, Anal. Bioanal. Chem. 372 (2002) 664.

[9] H. Du, M.D. Disney, B.L. Miller, T.D. Krauss, J. Am. Chem. Soc. 125 (2003) 4012.

[10] J.Y. Fang, C. Whitaker, B. Weslowski, M.S. Chen, J. Naciri, R. Shashidhar, J. Mater. Chem. 11 (2001) 2992.

[11] X. Feng, G.E. Fryxell, L.Q. Wang, A.Y. Kim, J. Liu, K.M. Kemner, Science 276 (1997) 923.

[12] J. Brown, L. Mercier, T.J. Pinnavaia, Chem. Commun. (1999) 69.

[13] M.H. Lim, C.F. Blanford, A. Stein, Chem. Mater. 10 (1998) 467.

[14] J.K. Yee, D.B. Parry, K.D. Caldwell, J.M. Harris, Langmuir 7 (1991) 307.

[15] J. Jia, B. Wang, A. Wu, G. Cheng, Z. Li, S. Dong, Anal. Chem. 74 (2002) 2217.

[16] W. Cheng, S. Dong, E. Wang, Langmuir 18 (2002) 9947.

[17] S. Park, M.J. Weaver, J. Phys. Chem. B 106 (2002) 8667.

[18] Y. Xiao, H.X. Ju, H.Y. Chen, Anal. Biochem. 278 (2000) 22.

[19] K.R. Brown, A.P. Fox, M.J. Natan, J. Am. Chem. Soc. 118 (1996) 1154.

[20] E. Lindner, S. Brugger, S. Steinbrecher, E. Plies, H.A. Mayer, J. Mater. Chem. 11 (2001) 1393.

[21] W. Jin, J.D. Brennan, Anal. Chim. Acta 461 (2002) 1.

[22] B.C. Dave, B. Dunn, J.S. Valentine, J.I. Zink, Anal. Chem. 66 (1994) A1120.

[23] B. Wang, B. Li, Q. Deng, S. Dong, Anal. Chem. 70 (1998) 3170.

[24] S. Mitra, S. Sampath, J. Mater. Chem. 12 (2002) 2531.

[25] M. Etienne, A. Walcarius, Talanta 59 (2003) 1173.

[26] P.N. Deepa, M. Kanungo, G. Claycomb, P.M.A. Sherwood, M.M. Collinson, Anal. Chem. 75 (2003) 5399.

[27] M. Kanungo, M.M. Collinson, Anal. Chem. 75 (2003) 6555.

[28] A. Walcarius, Chem. Mater. 13 (2001) 3351.

[29] S. Sayen, M. Etienne, J. Bessiere, A. Walcarius, Electroanalysis 14 (2002) 1521.

[30] A. Walcarius, M. Etienne, B. Lebeau, Chem. Mater. 15 (2003) 2161.

[31] J. Wang, P.V.A. Pamidi, D.R. Zanette, J. Am. Chem. Soc. 120 (1998) 5852.

[32] J.D. Badjic, N.M. Kostic, J. Mater. Chem. 11 (2001) 408.

[33] J.D. Badjic, N.M. Kostic, J. Phys. Chem. B 104 (2000) 11081.

[34] A.M. Becka, C.J. Miller, J. Phys. Chem. 96 (1992) 2657.

[35] J. Redepenning, H.M. Tunison, H.O. Finklea, Langmuir 9 (1993) 1404.

[36] R. Shacham, D. Avnir, D. Mandler, Adv. Mater. 11 (1999) 384.

[37] L.V. Protsailo, W.R. Fawcett, Langmuir 18 (2002) 8933.

[38] E. Sabatani, I. Rubinstein, J. Phys. Chem. 91 (1987) 6663.

[39] J. Liu, L. Zhang, N. Gu, J. Ren, Y. Wu, Z. Lu, P. Mao, D. Chen, Thin Solid Films 327 (1998) 176.

[40] L.L. Hench, J.K. West, Chem. Rev. 90 (1990) 33.